Land-atmosphere interactions in sub-polar and alpine climates in the CORDEX FPS LUCAS models: I. Evaluation of the snow-albedo effect

Anne Sophie Daloz[1], Clemens Schwingshackl[1,13], Priscilla Mooney[2], Susanna Strada[3], Diana Rechid[4], Edouard L. Davin[5], Eleni Katragkou[6], Nathalie de Noblet-Ducoudré[7], Michal Belda[8], Tomas Halenka[8], Marcus Breil[9], Rita M. Cardoso[10], Peter Hoffmann[4], Daniela C.A. Lima[10], Ronny Meier[5], Pedro M.M. Soares[10], Giannis Sofiadis[6], Gustav Strandberg[11], Merja H. Toelle[12] and Marianne T. Lund[1].

1. CICERO Center for International Climate Research, Oslo, Norway

2. NORCE Norwegian Research Centre, Bjerknes Centre for Climate Research, Bergen, Norway

3. International Center for Theoretical Physics, Trieste, Italy

4. Climate Service Center Germany, Helmholtz-Zentrum Hereon, Hamburg, Germany

5. Wyss Academy for Nature, Climate and Environmental Physics, Oeschger Center for Climate Change Research, University of Bern, Bern, Switzerland

6. Department of Meteorology and Climatology, School of Geology, Aristotle University of Thessaloniki, Thessaloniki, Greece

7. Laboratoire des Sciences du Climat et de l'environnement, Paris, France

8. Department of Atmospheric Physics, Faculty of Mathematics and Physics, Charles University, Prague, Czech Republic

9. Institute for Meteorology and Climate Research, Karlsruhe Institute of Technology, Karlsruhe, Germany

10. Instituto Dom Luiz, Faculdade de Ciências da Universidade de Lisboa, 1749-016 Lisboa, Portugal

11. Swedish Meteorological and Hydrological Institute, Norrkoping, Sweden

12. Center for Environmental Systems Research, University of Kassel, Germany

13. Department of Geography, Ludwig-Maximilians-Universität, Munich, Germany.

Corresponding author: Anne Sophie Daloz (anne.sophie.daloz@cicero.oslo.no)

Abstract

Seasonal snow cover plays a major role in the climate system of the Northern Hemisphere via its effect on land surface albedo and fluxes. In climate models the parameterization of interactions between snow and atmosphere remains a source of uncertainty and biases in the representation of local and global climate. Here, we evaluate the ability of an ensemble of regional climate models (RCMs) coupled to different land surface models to simulate snow-atmosphere interactions over Europe in winter and spring. We use a previously defined index, the Snow Albedo Sensitivity Index (SASI) to quantify the radiative forcing associated with snow cover anomalies. By comparing RCM-derived SASI values with SASI calculated from reanalyses and satellite retrievals, we show that an accurate simulation of snow cover is essential for correctly reproducing the observed forcing over mid- and high-latitudes in Europe. The choice of parameterizations, and primarily the choice of the land surface model, strongly influences the representation of SASI as it affects the ability of climate models to simulate snow cover accurately. The degree of agreement between the datasets differs between the accumulation and ablation periods, with the latter one presenting the greatest challenge for the RCMs. Given the dominant role of land surface processes in the simulation of snow cover during the ablation period, the results suggest that, during this time period, the choice of the land surface model is more critical for the representation of SASI than the atmospheric model.

1. Introduction

Snow is an important part of the climate system, regulating the temperature of the Earth's surface via its effect on surface albedo and surface fluxes. In mid- and high-latitude regions, snow is the main interface through which land interacts with the atmosphere during the cold season and the importance of snow-atmosphere interactions in modulating the energy budget at high latitudes during winter has been demonstrated (Diro and Sushama, 2018; Henderson et al., 2018; Xu and Dirmeyer, 2013a). Snow cover extent and depth can modify both surface energy and moisture budgets, triggering complex feedback mechanisms that impact both local and remote climates (Diro and Sushama, 2018). Reciprocally, with climate change, rising temperatures are already altering the Earth's snow amount and occurrences, shortening, for example, the snow season in Eurasia (Ye and Cohen, 2013; Gobiet et al., 2014; Mioduszewski et al., 2015; Beniston et al., 2018; Matiu et al., 2020). In this context, it is crucial to better understand snow-atmosphere processes and to evaluate the ability of climate models to represent them.

The direct impact of snow on the atmosphere is known as the snow albedo effect (SAE; Xu and Dirmeyer, 2013b), where the presence of snow affects the land surface energy budget and influences the local climate, modifying near-surface air temperature. The strength of the coupling between snow and the atmosphere is determined by processes involving radiative fluxes but also hydrology. Therefore, Xu and Dirmeyer (2013b) defined the snow hydrological effect (SHE), which includes the effects of soil moisture anomalies from snowmelt. Through land-atmosphere interactions, soil moisture anomalies have a delayed impact on the atmosphere. Besides these direct and indirect effects, positive and negative snow-atmosphere feedbacks, such as the snow-albedo feedback (SAF; Qu and Hall, 2007; Fletcher et al., 2015; Thackeray et al., 2018) can amplify or damp anomalies. The SAF represents changes in surface albedo from cooling (warming) that can cause decreases (increases) in absorbed solar radiation, amplifying the initial cooling (warming). Hence, SAF is an important driver for regional climate change in Northern Hemisphere land areas. Here, we focus on the one-way impact of snow on the atmosphere through SAE. To quantify the contribution from SAE to the snow-atmosphere coupling, Xu and Dirmeyer (2013b) developed the Snow Albedo Sensitivity Index (SASI). This index combines incoming

shortwave radiation with snow cover variability to quantify the snow-albedo coupling strength, i.e. SASI estimates the degree to which the radiative forcing responds to anomalies in snow cover. Applying SASI to satellite observations, Xu and Dirmeyer (2013b) found that the coupling between snow and albedo is particularly strong during the snowmelt period in the Northern Hemisphere. At high latitudes, for example, the effects of snow cover on the climate are strongly related to the way vegetation cover is prescribed. Removal of boreal forests locally reduces surface air temperature and precipitation by increasing surface albedo and decreasing plant evapotranspiration (Snyder et al. 2004).

While some previous studies have investigated snow-atmosphere processes in climate models for specific regions (e.g. European Alps; Magnusson et al., 2010; Diro et al. 2018; Matiu et al., 2019; Lüthi et al., 2019), the literature remains limited. Here, we build on earlier work from Xu and Dirmeyer (2011, 2013a,b), investigating the ability of an ensemble of regional climate models (RCMs) to represent snow cover and the radiative forcing associated with snow cover anomalies by evaluating SASI over Europe, including a comparison between mid- and high-latitude regions. We derive SASI using radiative fluxes and snow cover from satellites, reanalyses, and climate model outputs. We focus on winter and spring seasons, i.e. the accumulation and the ablation period, when SASI reaches its maximum. We use the RCMs outputs from the flagship pilot study Land Use and Climate Across Scale (LUCAS; Rechid et al., 2017; Breil et al., 2020; Davin et al., 2020; Reinhart et al., 2020; Sofiadis et al., 2021). LUCAS is endorsed by the Coordinated Regional Climate Downscaling Experiment (CORDEX) of the World Climate Research Programme (WCRP) over the European domain (EURO-CORDEX, Jacob et al., 2020) and it enables us to perform a broader assessment of several RCMs within a consistent framework. Our assessment is carried out in two parts and published in companion articles. In Part I, we investigate the ability of these RCMs to represent snow cover and SASI under present-day land cover distribution, while in Part II we explore the effects of large-scale changes in vegetation cover. In LUCAS, each RCM performed three coupled land-atmosphere experiments at the European scale: two idealized and intensive land use change experiments (GRASS and FOREST) and a control experiment (EVAL). The GRASS and FOREST experiments will be examined in the companion paper (Part II), while here we use simulations from the EVAL experiment only. Section 2 introduces the modelling and observational

datasets used in this study as well as the derivation of SASI, while Section 3 examines and discusses the ability of climate models to represent snow cover and SASI compared with satellite observations and reanalyses. Further, the origin of the differences in SASI between the models are explored by evaluating potential common biases in the ensemble of simulations as well as individual model biases. The analysis also explores the differences in SASI between mid- and high-latitude regions, opening the discussion on the impacts of different land cover for the simulation of SASI, which will be further explored in Part II. Finally, Section 4 offers some concluding remarks.

2. Data and methodology

2.1 LUCAS experiments and models

2.1.1 The LUCAS experiments

The simulations from the flagship pilot study LUCAS cover the standard EURO-CORDEX domain (Jacob et al., 2014) with a horizontal grid resolution of 0.44° (around 50 km). All RCMs in LUCAS, except the RegCM model, use a rotated coordinate system, which is a cartographic projection to transform coordinates from a 3D sphere to a 2D plane (the model domain). The RegCM model applies a Lambert conformal projection (suitable for mid-latitudes) on a regular grid. Here we use outputs from the EVAL experiment, which employ standard land use and land cover maps. All simulations span the period 1986–2015 (with a spin-up period ranging from one up to six years depending on the model) and take lateral and boundary conditions from the ERA-Interim reanalysis (Dee et al., 2011). More details can be found in Davin et al. (2020).

2.1.2 Models and configurations

We use the outputs from ten coupled surface-atmosphere RCM simulations that participated in the LUCAS project and were available at the time when we performed the analysis. The main model characteristics that are important for snow albedo coupling are summarized in Table 1, while a detailed description of the RCMs is provided by Davin et al. (2020). The model ensemble presents five different RCMs: COSMO-CLM version 5.0-clm9 (Sørland et al., 2021), WRF version 3.8.1 (Skamarock et al., 2008), RegCM versions 4.6 and 4.7 (Giorgi et al., 2012), RCA4 (Strandberg et al., 2015) and REMO (Jacob et al., 2012). These RCMs contributed with different setups and configurations as described in

Table 1. For example, the same RCM is coupled to different land surface models (LSMs): COSMO-CLM is coupled to three distinct LSMs, which are CLM5.0 (Lawrence et al., 2020), VEG3D (Breil and Schadler, 2017) and TERRA-ML (Schrodin and Heise, 2002). WRF is coupled with either CLM4.0 (Oleson et al., 2010) or NOAH-MP (Niu et al., 2011). Vice versa, the same LSM is combined with different versions of RCMs. The LSM CLM4.5 (Oleson et al., 2013) is coupled to two distinct versions of RegCM (4.6 and 4.7) which also differ in their choice of convection schemes. There are also two ensemble members where the same RCM and LSM are used (WRF and Noah-MP) but with different planetary boundary layer (PBL) schemes; these are named WRFa-NoahMP and WRFc-NoahMP in Table 1. The time resolution at which model outputs have been stored, varies from one variable to another and follows the CORDEX protocol. For the analyses in the present study, we use daily and monthly model outputs for incoming shortwave radiation and snow cover. For deriving SASI, the native grid of the models was kept, minimising data loss. The other fields were interpolated to a common 0.5°x0.5° grid using Climate Data Operators (CDO) bilinear remapping.

2.1.3 Snow schemes across different land surface models

At high latitudes, the effects of snow cover on regional climate are strongly modulated by vegetation cover. The important role of forest albedo on winter and spring climate in the high-latitudes is highlighted by bothfield campaigns, such as the Boreal Ecosystem-Atmosphere Study (BOREAS; Betts et al., 2001), and modeling studies (e.g., Betts and Ball, 1997; Betts et al., 1996; Betts et al., 2001; Bonan, 2008; Davin and Noblet-Ducoudré, 2010; Mooney et al., 2021), which led to the implementation of more sophisticated snow sub-models in LSMs that account for the burial of vegetation by snow. All LSMs in the LUCAS ensemble derive the fraction of vegetation buried by snow, adopting similar approaches that account for snow depth, vegetation height and snow cover fraction. The snow cover fraction f_{sno} depends on the snow cover accumulated at the surface over bare soil or vegetation and influences the calculation of surface albedo and fluxes. Canopy-intercepted snow does not contribute to the snow cover fraction at the ground. The CLM models (CLM4.0, CLM4.5 and CLM5.0; Swenson and Lawrence, 2012) and the internal LSM of the RCA4 model (Samuelsson et al., 2015) separately calculate the snow cover fraction during snowfall and snow melting processes, accounting for sub-grid orography

when snow melting occurs. In Noah-MP, the snow cover fraction depends on snow depth, ground roughness length and snow density (Niu and Yang, 2004). In VEG3D, the snow cover fraction is internally calculated as a function of snow depth and vegetation height, and is used to update surface parameters, such as albedo. However, since f_{sno} is not a default model output in VEG3D, the snow cover fraction has been computed for analysis purpose as a snow flag in case of a snow height above a certain threshold, producing a value that is equal to one or zero (i.e., the grid box is covered by snow or not).

Some LSMs are more sophisticated than others. CLM5.0 (Lawrence et al., 2020) and Noah-MP (Niu et al., 2007) separately treat canopy-intercepted snow and more realistically capture temperature and wind effects on snow processes. In addition, LSMs differ in the number of additional layers for snow calculation: CLM5.0 uses 12 snow layers; CLM4.0, CLM4.5 and TERRA-ML (Tolle et al., 2018) use five; Noah-MP uses three; VEG3D and iMOVE use two; and RCA4 uses one. The iMOVE model adopts the snow parameterisation from the global climate model ECHAM4 (Roeckner, et al., 1996) and reproduces the snow albedo as a linear function of the snow surface temperature and of the forest fraction in a grid cell, with fixed maximum and minimum snow albedo at temperatures lower than -10°C and at 0°C, respectively (Kotlarskis, 2007). In the VEG3D model, the snow scheme is based on the Canadian Land Surface Scheme (CLASS) (Verseghy, 1991) and ISBA (Douville et al., 1995) and accounts for changes of surface albedo and emissivity as well as processes like compaction, destructive metamorphosis, the melting of snow, and the freezing of liquid water. The TERRA-ML LSM model is a bulk/1D LSM that applies an infinitesimal vegetation layer on top of the soil surface and has no canopy (i.e., vegetation lays flat on the surface). Therefore, the snow always stays on top of the vegetation and there is no snow under the trees. To correctly reproduce the effect on radiation of trees masking the ground snow, TERRA-ML applies a reduction factor for the snow albedo when vegetation (e.g., forest canopies) masks the snow.

2.2 Reanalyses and remote sensing data

Reanalysis data from ERA5-Land (Muñoz Sabater, 2019; Muñoz Sabater et al., 2021) and MERRA-2 (Gelaro et al., 2017) as well as satellite data from the Moderate Resolution Imaging Spectroradiometer (MODIS; Hall and Riggs, 2016) are used to evaluate the modelled snow distribution

and radiation in the RCMs. Specifically, we use monthly data for snow cover and incoming shortwave radiation from ERA5-Land and MERRA-2, and daily snow cover data from the MODIS sensors AQUA (MYD10C1) and TERRA (MOD10C1). The reanalysis data are interpolated bilinearly to the common 0.5°x0.5° grid. Reanalysis data cover the time period 1986-2015 and MODIS data the period 2003-2015. Only MODIS-AQUA data are displayed in the main figures of the article, while data from MODIS-TERRA are included in the supplemental material.

For MODIS data, the following processing steps are applied:

1. Since heavy cloud cover prevents a correct estimation of snow cover, data are masked by applying a threshold of 50% to the percent of clouds in each grid cell. For comparison, we also show the results when applying a threshold of 20% in Supplementary Figure S1.

2. Only data flagged as "best", "good", and "ok" are used while all other data are masked.

3. Data are conservatively remapped to the common 0.5°x0.5° grid. Conservative remapping is chosen due to the large difference in resolution between the original MODIS data (0.05°) and the target grid (0.5°), as it considers all grid points in the interpolation while, e.g., bilinear interpolation would only consider the neighbouring grid cells of the target grid.

4. A land-sea mask is applied to make sure that only land grid points are included in the analysis. Only grid points with more than 50% land fraction are included.

5. Data are averaged to monthly resolution.

2.3 Snow Albedo Sensitivity Index (SASI) and geographical scope

SASI is an index that quantifies the climate forcing due to the snow albedo effect (Xu and Dirmeyer, 2013b). It is defined as:

$$SASI = SW * \sigma(f_{sno}) * \Delta\alpha \qquad (1)$$

where SW is the incident shortwave radiation at the surface, $\sigma(f_{sno})$ is the standard deviation of snow cover fraction, which represents the interannual variation of monthly-mean snow cover values, and $\Delta\alpha$ is the average difference between the albedo of a snow-covered surface and the albedo of a snow-free surface. $\Delta\alpha$ is a constant value of 0.4 as assumed in Xu and Dirmeyer (2013b). SASI is given in Wm^{-2}

and high values of SASI, such as 10 Wm^{-2}, indicate a strong climate forcing from the snow albedo effect (Xu and Dirmeyer, 2013b).

To better understand geographical differences in the role of snow for land-atmosphere coupling, we focus on three sub-regions over Europe, with different climate, vegetation cover, topography and latitudes: Scandinavia [5ºE-30ºE, 55ºN-70ºN], East Europe [16 ºE-30ºE, 44ºN-55ºN] and East Baltic [20ºE-40ºE, 50ºN-62ºN] (see Figure 1). The first two regions, Scandinavia and East Europe correspond to regions 8 and 5 of the PRUDENCE project (Prediction of Regional scenarios and Uncertainties for Defining EuropeaN Climate change risk and Effects; Christensen and Christensen, 2007). The three selected regions differ in terms of climate but also in terms of vegetation: needle-leaved evergreen forests dominate in Scandinavia while cropland and more deciduous trees cover the other two regions. The Scandinavian region also stands out because of its geographical location stretching over high latitudes, where the incoming shortwave radiation is very small or zero during winter. In comparison with the plain region of the East Baltic region, East Europe and Scandinavia have a more complex topography as they encompass the Carpathian and Scandinavian mountains, respectively.

3. Results and discussion

3.1 Snow cover in Europe from satellites, reanalyses and RCMs

We start by giving an overview of spatiotemporal differences in snow cover between the different datasets. Figure 2 shows the geographical distribution of snow cover over Europe from January to June based on satellite observations averaged over the 2003-2015 period, and data from ERA5-Land, MERRA2 and the LUCAS models, averaged over 1986-2015. The same figure with all datasets averaged over the time period 2003-2015 is presented in the Supplemental Material, Figure S2. MODIS-AQUA, ERA5-Land, and MERRA2 all show a similar spatiotemporal cycle, albeit with some differences in amplitude, e.g. higher snow cover in spring in ERA5-land compared to the MODIS-AQUA and MERRA-2. Snow cover is high during the first months of the year when snow is accumulating (accumulation period), and then decreasing when snow is melting (ablation period). The satellite and reanalysis datasets capture the later snow melt at higher latitudes than at mid-latitudes, showing high snow cover values during spring, while over the rest of Europe snow cover values are very

low. Most of the models exhibit the same overall spatiotemporal cycle in snow cover. However, large differences exist across models regarding the amplitude and pattern of snow cover, especially during the ablation period. To facilitate further investigations into inter-model differences, we consider models by atmospheric model groups (i.e., WRF, CCLM, RegCM, and others), highlighted by the different colours in the labels of Figure 2. Large dissimilarities can appear between the members of each group. For example, in the WRF model group, WRFb-CLM4.0 has much higher values in snow cover than the other members. This is also the case for the CCLM group, with CCLM-VEG3D showing higher snow cover values than the rest of the CCLM models. For the RegCM group, the differences between the two group members are less pronounced. Comparing across atmospheric model groups shows that RegCM models tend to have snow staying longer on the ground, with higher values in snow cover in May and June compared to the other models. Generally, the comparison between the different atmospheric model groups indicates that using the same atmospheric model does not guarantee producing a similar representation of snow cover, emphasizing that the specificities of each configuration (e.g. parameterization, land surface model) can have a large impact on the representation of snow variables. These dissimilarities are not limited to snow cover and applies to other variables such as snow depth, which also exhibit large inter-model differences (see. Supplemental Material, Figure S3). Such variations can have large effects on the representation of the local climate through, for example, the impact on the surface energy budget.

3.2 SASI in satellite observations, reanalyses and RCMs over Europe

Figure 3 shows the geographical distribution of SASI over Europe from January to June for satellite observations (2003-2015), ERA5-Land, MERRA-2, and the LUCAS models (1986-2015). Focusing first on the satellite observations, MERRA-2 and ERA5-Land, an increase in SASI can be observed during the first months of the year when solar radiation increases, and snow accumulates. The maximum is reached during the ablation period in March or April, depending on the region examined, and finally SASI decreases as snow completely melts. At higher latitudes snow melts later than at mid-latitudes (see Figure 2), causing high SASI values during spring. The SASI maximum shows a rather sharp peak in East Baltic, while it is more spread out in East Europe and in Scandinavia. This overall

seasonal trend is consistent with Xu and Dirmeyer (2013b). Most of the models exhibit a similar spatiotemporal cycle in SASI as the satellite observations, ERA5-Land, and MERRA-2. However, large differences can be seen across models in terms of pattern and amplitude. In March over the Carpathian Mountains, for example, SASI varies between 1 Wm^{-2} for WRFa-NoahMP and RCA, and 10 Wm^{-2} for CCLM-CLM5.0 and RegCMa-CLM4.5. It is also noteworthy that for almost all the models, SASI is close to zero everywhere in continental Europe in May and June except for RegCMb-CLM4.5 and CCLM-VEG3D, which still have high values of SASI (~10 Wm^{-2}).

In each atmospheric model group, simulations show large dissimilarities in terms of SASI, in amplitude or pattern, especially during the ablation period. WRFa-NoahMP and WRFc-NoahMP show noticeable differences in the amplitude and pattern of SASI (Fig. 3), even though they use the same LSM and atmospheric model. The differences come from their distinct parameterizations of planetary boundary layer and convection, affecting the simulated temperature and precipitation, which in return can influence their representation of snow cover and SASI. This demonstrates the importance of atmospheric processes and their model representation for representing snow processes. Furthermore, when WRF is coupled with the LSM CLM4.0 (WRFb-CLM4.0) it shows different results compared to the simulations with Noah-MP. In WRFa-NoahMP snow melts about one month earlier than in WRFb-CLM4.0. Such dissimilarities also exist in the RegCM and CCLM groups. CCLM-CLM5.0, CCLM-TERRA, and CCLM-VEG3D use the same RCM but different LSMs. However, in contrast to the two other CCLM configurations, CCLM-VEG3D uses a snow flag for snow cover (i.e., only indicating if snow is present or not; Section 2.3), likely explaining its different representation of SASI. This suggests that SASI is very sensitive to the model configurations and process parameterizations. In particular, the choice of the LSM or certain parameterizations (e.g. the convection scheme) can strongly influence the representation of the climate forcing from the snow albedo effect. The role of the LSM in this context will be investigated further below.

3.3 Investigating the origin of the differences in the representation of SASI

3.3.1 Transition between the accumulation and ablation periods

To further investigate the differences in snow albedo coupling strength between the simulations and the observation-based datasets during the accumulation and ablation periods, a time-series of SASI from January to June is presented in Figure 4 for the three sub-regions East Europe, East Baltic and Scandinavia (see Figure 1 for their extents). SASI values are generally higher in East Europe and East Baltic (mid-latitude regions) than in Scandinavia (high-latitude region). This confirms previous findings from Xu and Dirmeyer (2013b), which estimated higher values of SASI in mid- versus high-latitude regions in satellite observations. Part of this difference is likely due to the lower values in incoming solar radiation in Scandinavia compared to the other regions. However, even with lower SASI values at high- versus mid-latitudes, this result suggests that the radiative forcing due to the snow albedo effect is not negligible over high-latitude regions in winter and spring, highlighting the importance of snow-atmosphere processes in mid- and high-latitudes in the Northern hemisphere.

Returning to the comparison of the different datasets, the models and observations indicate a pronounced springtime peak in SASI in all three regions. As already mentioned, the maximum in SASI occurs during the ablation period, when snow is melting. The exact timing of this transition depends on the latitude of the respective region. There is also a difference in the timing of the peak between the satellite observations, MERRA-2, and ERA5-Land, in particular over Scandinavia and East Baltic, although the amplitude is very similar. Over East Europe the peak occurs in March for both the satellite observations, and ERA5-Land but in February for MERRA-2, for East Baltic in March (satellites, MERRA-2) or April (ERA5-Land), and for Scandinavia in April (satellites, MERRA-2) or May (ERA5-Land). The origin of these differences remains unclear, but it is not related to the difference in time period between the satellite observations and the reanalysis (see Figure S2 for snow cover).

The LUCAS simulations also show a pronounced peak in SASI in all regions (Fig. 3), however they do not all agree on the timing and the amplitude of the signal. This is true both within the different groups of models but also for all the simulations. For example, in the East Baltic region, some models (WRFc-NoahMP and WRFa-NoahMP) simulate a peak in March, others in April (WRFb-CLM4.0 and CCLM-CLM5.0) or even in May (RegCMb-CLM4.5 and CCLM-VEG3D). In general, RegCMb-CLM4.5 and CCLM-VEG3D tend to present the latest peak in SASI as well as the highest amplitude in the signal. On the other hand, WRFa-NoahMP tends to produce an earlier peak and lower values of

SASI, especially over East Europe. These differences might be related to snow remaining longer on the ground (Section 3.1), and melting later in the different models, and will be further explored in the next section. More generally, we see that during the accumulation period, all the datasets are in better agreement compared to the ablation period (Fig. 4). For East Europe and East Baltic, the spread largely increases in March and for Scandinavia from April until the end of the season, when the snow is melting.

This large model spread during the ablation period is further confirmed by examining the pattern correlation between the simulations and ERA5-Land from January to June (not shown). For many models, the correlation is high at the beginning of the season but strongly decreases in March or April, when the snow starts melting. These results agree with previous studies showing the difficulties of climate models to represent snow processes during the ablation period (Essery et al. 2009). Given the dominant role of land surface over atmospheric processes during the ablation period, this suggests that the choice of the LSM is more critical for the representation of the climate forcing from the snow albedo effect than the atmospheric model in spring. For simulating snow-covered areas at different stages of ablation, a correct representation of the landscape type is important (Pomeroy et al., 1998). In this context, it is interesting that no systematic differences can be observed between the PFT-dominant versus PFT-tile models representation of the sub-grid scale surface heterogeneity (Table 1); as it does not seem to affect the ability of RCMs to represent snow cover or SASI. The pattern correlation (not shown) also indicates that the behaviour of the RCMs is different between East Europe and East Baltic versus Scandinavia. Over the latter region, most RCMs differ from the reanalysis, as indicated by low correlations. Earlier studies showed that snow accumulates or melts very differently in an open region compared to a forested region (Jonas and Essery, 2014; Moeser et al., 2016). Our results suggest that RCMs represent snow processes better in open spaces like the East Baltic than in forest-covered regions like Scandinavia. The relationship between the representation of SASI and land cover will be further explored in the companion article, Part II. The mountains in Scandinavia could also be a source of biases since the resolution of the RCM simulations (0.44°) can be considered insufficient to represent the more complex topography of Scandinavia.

3.3.2 Inter-model differences in SASI

To better understand the origin of the differences in SASI across RCMs, we explore the relationship between SASI and its components, surface snow cover and shortwave radiation, during the accumulation and ablation periods. Figure 5 presents a comparison of monthly surface snow cover for the LUCAS simulations, MERRA-2, ERA5-Land, and MODIS-AQUA, averaged over the three regions of interest, from January to May. As shown in Section 3.1, differences can be observed between the reanalyses and the satellite observations as these datasets have their own limitations or biases. For example, as each reanalysis dataset is based on a different dynamical core, each model may parameterize or resolve physical processes differently (Daloz et al. 2020). The surface snow cover in East Baltic in March is ~0.6 for MODIS, ~0.7 for MERRA-2 and ~0.8 for ERA5-Land. It is therefore important to include several reference datasets to evaluate the ability of climate models to represent snow cover and estimate the uncertainties associated with this variable. Based on Figure 4, RegCMb-CLM4.5 and CCLM-VEG3D were identified as models with higher values in SASI during the ablation period and later peaks for all regions. Figure 5 shows that this behaviour can be at least partly attributed to their representation of snow cover. During the ablation period, both tend to produce higher values of snow cover compared to the other models and to keep high values later in the season, when they lie completely outside the range of the reference datasets (indicated by the black dots in Figure 5). This is particularly striking for CCLM-VEG3D. Similarly, the low SASI peaks for WRFa-NoahMP, which also occur earlier than the peaks for other models (Figure 4), might be related to the comparatively low values in snow cover (WRFa-NoahMP lying outside the range of the reference datasets in all months and all regions) and the small interannual snow cover variability compared to the other RCMs, particularly in East Europe (Figure 5). The differences in snow cover are also reflected by the timing of snowmelt (reduction in snow mass) for the different RCMs (Supplemental Material; Figure S4). The models having high snow cover late in spring (RegCMb-CLM4.5 and CCLM-VEG3D) tend to have later snow melt than the other models while WRFa-NoahMP, showing reduced snow cover earlier than the other models, also tends to have an earlier snowmelt.

Another component of SASI is shortwave radiation at the surface, shown in Figure 6 for the LUCAS simulations and MERRA-2 and ERA5-Land, averaged over our three regions of interest, from January to May. The comparison between the RCMs and the reanalysis shows noticeable differences

for some models. Both REMO-iMOVE and WRFa-NoahMP exhibit very different results in terms of surface shortwave radiation compared to the datasets, showing much lower and higher values than the reference datasets, respectively. However, even with these discrepancies, they both reproduce SASI reasonably well.

This is confirmed by Figure 7 showing the average correlation across models between SASI and shortwave radiation (left) as well as SASI and snow cover (right) for the LUCAS models. Scandinavia and East Baltic present similar results with significant, positive correlations between SASI and snow cover for almost all months, associated with positive but not statistically significant correlations between SASI and shortwave radiation. For East Europe, the correlation between SASI and snow cover is lower and not significant in January and February but remains high and significant the rest of the time period. In parallel, the correlation between SASI and downward shortwave radiation at the surface is negative for almost all months (but not statistically significant). Overall, high and significant correlations often appear between SASI and snow cover for the three regions from January to June. On the other hand, the correlations between SASI and shortwave radiation are low and usually not significant. This indicates that the differences in the representation of the forcing from the snow albedo effect are mostly driven by differences in the representation of snow cover in the models.

4. Conclusion

Previous work has demonstrated the difficulty for climate models to represent snow variables or processes, such as snow cover and depth (Matiu et al., 2020) or snow-atmosphere processes such as the snow-albedo feedback (SAF; Fletcher et al., 2015), but the origin of the differences between models is not clear yet. In this work, we focus on the ability of RCMs to simulate the radiative forcing associated with snow cover anomalies in winter and spring over Europe and explore the origin of the differences across the RCMs. The radiative forcing associated with snow cover anomalies is represented by the index SASI (Xu and Dirmeyer, 2013b), which quantifies the strength of the coupling between snow and surface net shortwave radiation. Ten RCMs from the CORDEX Flagship Pilot Study LUCAS are compared to satellite observations and the reanalysis datasets ERA5-Land and MERRA-2. These simulations are part of the control experiment of LUCAS.

The results show that climate models are able to reproduce well some of the SASI characteristics (e.g. existence of a peak, amplitude of the peak) compared to reanalyses and satellite observations, even if large differences appear between the RCMs, for all groups of models. The climate models' ability to represent SASI is highly related to their representation of snow cover, which can be difficult to represent for climate models. Our results also suggest that the models' capability highly differs between the accumulation and ablation periods. Most models have much lower agreement with reanalyses and satellite observations in the ablation period, indicating a systematic bias regarding snow cover in spring, in turn pointing towards a bias from LSMs. This bias seems to be common to most LSMs even if they are based on different assumptions and parameterizations. It is also interesting that even though CCLM-TERRA is not as advanced in terms of snow modelling compared to the other models, it still manages to represent SASI reasonably well over Europe. In addition, there were no systematic differences between the PFT-dominant versus PFT-tile models (Table 1) as it does not seem to affect the ability of RCMs to represent snow cover or SASI. Taking advantage of the different configurations of the LUCAS simulations, we have also explored the role of distinct parts of the models in their ability to represent SASI. This work has emphasized the role of the LSMs, but other components can also play an important role. For example, WRFc-NoahMP and WRFa-NoahMP, even though using the same RCM and LSM, show noticeable differences in the amplitude and pattern of SASI. Their differences in parameterizations (planetary boundary layer and convection) are certainly affecting the way they represent SASI, highlighting the impact of such choices and the role of atmospheric processes.

Mid- and high-latitude areas are also specifically examined looking at three sub-regions: Scandinavia, East Europe and East Baltic. The comparison of the three sub-regions shows the difficulties for models to simulate SASI over Scandinavia during the accumulation and ablation periods. The simulation of snow processes in a forested region is more challenging than in an open region (Jonas and Essery, 2014; Moeser et al., 2016). Thus, climate models can potentially have more difficulties representing snow processes in forest-covered regions like Scandinavia compared to open-land regions like East Baltic. The relationship between the representation of SASI and land-cover will be further explored in the companion article (Part II), analyzing the other LUCAS experiments GRASS and FOREST. Finally, the comparison of mid- versus high-latitude regions shows slightly higher values of

SASI over the mid-latitude regions in satellite observations, ERA5-Land, MERRA-2, and most of the RCMs. This confirms previous findings from Xu and Dirmeyer (2013b), which estimated higher values of SASI in mid- versus high-latitude regions in satellite observations. Our results also suggest that the climate forcing due to the snow albedo effect is not negligible over high-latitude regions in winter and spring. This is important since often the land-atmosphere coupling is considered weaker at higher latitudes) but it is also possible that this coupling happens through snow and is therefore underestimated.

Although it is difficult to identify the origin of the bias in the RCMs, an increase in spatial resolution might improve the simulation of snow cover and therefore the representation of SASI. For example, over Scandinavia, an increase in spatial resolution would provide a better representation of the complex topography of the region as well as its forested areas, which may lead to an improved simulation of the coupling between snow and albedo. The coming phases of LUCAS could help answer this question as they will produce simulations at higher spatial resolutions (12 km in phase 2 and convection-permitting (<3km) in phase 3).

Competing interests: The authors declare that they have no conflict of interest.

Data availability: All raw data can be provided by the corresponding author upon request.

Authors contribution: ASD, CS, PM, MTL and SS wrote the manuscript draft, which has been reviewed and edited by all the co-authors.

Acknowledgements

CICERO researchers acknowledge funding from the Norwegian Research Council (grant 254966). In Norway, the simulations were stored on the server NIRD with resources provided by UNINETT Sigma2 - the National Infrastructure for High Performance Computing and Data Storage in Norway. WRFc-NoahMP simulations were performed and stored on resources provided by UNINETT Sigma2 - the National Infrastructure for High Performance Computing and Data Storage in Norway (NN9280K,

NS9001K, NS9599K). WRFb-CLM4.0 simulations were supported by computational time granted from the National Infrastructures for Research and Technology S.A. (GRNET S.A.) in the National HPC facility - ARIS - under project ID pr005025 and pr007033_thin. Edouard L. Davin and Ronny Meier acknowledge financial support from the Swiss National Science Foundation (SNSF) through the CLIMPULSE project and thank the Swiss National Supercomputing Centre (CSCS) for providing computing resources. P. Hoffmann is funded by the Climate Service Center Germany (GERICS) of the Helmholtz-Zentrum Hereon in the frame of the Helmholtz-Institut Climate Service Science (HICSS) project LANDMATE. M. Belda and T. Halenka acknowledge support by The Ministry of Education, Youth and Sports from the Large Infrastructures for Research, Experimental Development and Innovations project "IT4Innovations National Supercomputing Center – LM2015070" and the INTER-EXCELLENCE program LTT17007, and support by Charles University from the PROGRES Q16 program. The authors gratefully acknowledge the WCRP CORDEX Flagship Pilot Study LUCAS "Land use and Climate Across Scales" and the research data exchange infrastructure and services provided by the Jülich Supercomputing Centre, Germany, as part of the Helmholtz Data Federation initiative. R. M. Cardoso, D. C. A. Lima P. M. M. Soares were supported by national funds through FCT (Fundação para a Ciência e a Tecnologia, Portugal) under project LEADING (PTDC/CTA-MET/28914/2017), and project UIDB/50019/2020. This study contains modified Copernicus Climate Change Service Information 2021. ERA5-Land data are available at https://doi.org/10.24381/cds.e2161bac and https://doi.org/10.24381/cds.68d2bb30. The information related to GlobSnow data is presented in https://doi.org/10.1016/j.rse.2014.09.018. Variables from MERRA2 have been downloaded in 2019 and 2020 via NASA/GSFC, Greenbelt, MD, USA, NASA Goddard Earth Sciences Data and Information Services Center (GES DISC).

References:

Beniston, M., Farinotti, D., Stoffel, M., Andreassen, L.M., Coppola, E., Eckert, N., Fantini, A., Giacona, F., Hauck, C., Huss, M., Huwald, H., Lehning, M., López-Moreno, J.I., Magnusson, J., Marty, C., Morán-Tejéda, E., Morin, S., Naaim, M., Provenzale, A., Rabatel, A., Six, D., Stötter, J., Strasser,

U., Terzago, S., Vincent, C., The European mountain cryosphere: A review of its current state, trends, and future challenges, Cryosphere, 12 (2), pp. 759-794, 2018.

Betts, A. K., Ball, J. H., Beljaars A. C. M., Miller, M. J. and Viterbo, P. A.: The land surface-atmosphere interaction: A review based on observational and global modeling perspectives, Journal of Geophysical Research: Atmospheres. 101(D3), 7209-7225, 10.1029/95jd02135, 1996.

Betts, A. K. & Ball, J. H.: Albedo over the boreal forest, Journal of Geophysical Research: Atmospheres. 102(D24), 28901-28909, 10.1029/96jd03876, 1997.

Betts, A. K., Ball, J. H. and McCaughey, J. H.: Near-surface climate in the boreal forest, Journal of Geophysical Research: Atmospheres. 106(D24), 33529-33541, 10.1029/2001jd900047, 2001.

Bonan, G. B.: Forests and Climate Change: Forcings, Feedbacks, and the Climate Benefits of Forests, Science. 320(5882), 1444-1449, 10.1126/science.1155121, 2008.

Braun, F. J., & Schädler G.: Comparison of soil hydraulic parameterizations for mesoscale meteorological models. Journal of Applied Meteorology, 44(7), 1116-1132, 2005.

Breil, M., & Schädler, G.: Quantification of the uncertainties in soil and vegetation parameterizations for regional climate simulations in Europe. Journal of Hydrometeorology, 18(5), 1535-1548, 2017.

Breil, M., Rechid, D., Davin, E, de Noblet-Ducoudré, N., Katragou, E., Cardoso, R., Hoffmann P., Jach, L., Soares, P., Sofiadis, G., Strada, S., Strandberg, G., Toelle, M., Warrach-Sag, K.: The opposing effects of afforestation on the diurnal temperature cycle at the surface and in the atmospheric surface layer in the European summer. Journal of Climate, 33 (21), pp. 9159-9179, 2020.

C3S: Copernicus Climate Change Service (C3S) (2017): ERA5: Fifth generation of ECMWF atmospheric reanalyses of the global climate. Copernicus Climate Change Service Climate Data Store (CDS), date of access 200414. https://cds.climate.copernicus.eu/cdsapp#!/home, 2017.

Christensen, J.H., and Christensen, O.B.: A summary of the PRUDENCE model projections of changes in European climate by the end of this century. Climatic Change 81, 7–30,. https://doi.org/10.1007/s10584-006-9210-7, 2007.

Daloz, A. S., Mateling, M., L'Ecuyer, T., Kulie, M., Wood, N. B., Durand, M., Wrzesien, M., Stjern, C. W., and Dimri, A. P.: How much snow falls in the world's mountains? A first look at mountain snowfall estimates in A-train observations and reanalyses, The Cryosphere, 14, 3195–3207, https://doi.org/10.5194/tc-14-3195-2020, 2020.

Davin, E. L., & Noblet-Ducoudré, N. D.: Climatic Impact of Global-Scale Deforestation: Radiative versus Nonradiative Processes, Journal of Climate. 23(1), 97-112, 10.1175/2009jcli3102.1, 2010.

Davin, E. L., Rechid, D., Breil, M., Cardoso, R. M., Coppola, E., Hoffmann, P., Jach, L. L., Katragkou, E., de Noblet-Ducoudré, N., Radtke, K., Raffa, M., Soares, P. M. M., Sofiadis, G., Strada, S., Strandberg, G., Tölle, M. H., Warrach-Sagi, K. & Wulfmeyer, V.: Biogeophysical impacts of forestation in Europe: first results from the LUCAS (Land Use and Climate Across Scales) regional climate model intercomparison, Earth Syst. Dynam. 11(1), 183-200, 10.5194/esd-11-183-2020, 2020.

Deardorff, J.: Efficient prediction of ground surface temperature and moisture, with inclusion of a layer of vegetation, J. Geophys. Res, 83(4), 1889 –1903, doi:10.1029/JC083iC04p01889, 1978.

Dee, D. P., Uppala, S. M., Simmons, A. J., Berrisford, P., Poli, P., Kobayashi, S., Andrae, U., Balmaseda, M. A., Balsamo, G., Bauer, P., Bechtold, P., Beljaars, A. C. M., van de Berg, L., Bidlot, J., Bormann, N., Delsol, C., Dragani, R., Fuentes, M., Geer, A. J., Haimberger, L., Healy, S. B., Hersbach, H., Hólm, E. V., Isaksen, L., Kållberg, P., Köhler, M., Matricardi, M., McNally, A. P., Monge-Sanz, B. M., Morcrette, J.-J., Park, B.-K., Peubey, C., de Rosnay, P., Tavolato, C., Thépaut, J.-N., & Vitart, F.: The ERA-Interim reanalysis: configuration and performance of the data assimilation system, Quarterly Journal of the Royal Meteorological Society. 137(656), 553-597, 10.1002/qj.828, 2011.

Diro, G. T., & Sushama, L.: Snow–precipitation coupling and related atmospheric feedbacks over North America, Atmospheric Science Letters. 19(8), e831, 10.1002/asl.831, 2018.

Diro, G.T., Sushama, L. and Huziy, O. Snow-atmosphere coupling and its impact on temperature variability and extremes over North America. Clim Dyn 50, 2993-3007, https://doi.org/10.1007/s00382-017-3788-5, 2018.

Doms, G., Förstner, J., Heise, E., Herzog, H.-J., Mironov, D., Raschendorfer, M., Reinhardt, T., Ritter, Schrodin, B.R., Schulz, J.-P., Vogel G.: A Description of the Nonhydrostatic Regional Model LM, Part II: Physical Parameterization. DWD, 2013.

Douville, H., J-F. Royer, and J-F. Mahouf: A new snow parameterization for the Meteo-France climate model. Part I: Validation in stand-alone experiments. Climate Dyn. 12:21–35, 1995.

Essery, R., and co-authors: SNOWMIP2: An Evaluation of Forest Snow Process Simulations. Bull. Amer. Meteor. Soc., **90**, 1120–1136, https://doi.org/10.1175/2009BAMS2629.1, 2009.

Fletcher, C. G., Thackeray, C. W., and Burgers, T. M.: Evaluating biases in simulated snow albedo feedback in two generations of climate models, J. Geophys. Res. Atmos., 120, 12– 26, doi:10.1002/2014JD022546, 2015.

Gelaro R., McCarty W., Suárez M. J., Todling R., Molod A., Takacs L., Randles C. A., Darmenov A., Bosilovich M. G., Reichle R., Wargan K., Coy L., Cullather R., Draper C., Akella S., Buchard V., Conaty A., Silva A. M. d., Gu W., Kim G.-K., Koster R., Lucchesi R., Merkova D., Nielsen J. E., Partyka G., Pawson S., Putman W., Rienecker M., Schubert S. D., Sienkiewicz M. & Zhao B.: The Modern-Era Retrospective Analysis for Research and Applications, Version 2 (MERRA-2), Journal of Climate. 30(14), 5419-5454, 10.1175/jcli-d-16-0758.1, 2017.

Giorgi F., Coppola, E., Solmon, F., Mariotti, L., Sylla, M.B., Bi, X., Elguindi, N., Diro, G.T., Nair, V., Giuliani, G., Turuncoglu, U.U., Cozzini, S., Güttler, I., O'Brien, T.A., Shalaby A. Tawfik, A. B., Zakey, A.S., Steiner, A.L., Stordal, F., Sloan, L.C., & Brankovic C.: RegCM4: model description and preliminary tests over multiple CORDEX domains. Clim. Res., 52:7–29. doi: 10.3354/cr01018, 2012.

Grabe, F.: Simulation der Wechselwirkung zwischen Atmosphäre, Vegetation und Erdoberfläche bei Verwendung unterschiedlicher Parametrisierungsansätze. PhD Thesis. Inst. for Meteorology and Climate Research, Karlsruhe Institute of Technology, Karlsruhe, Germany, 2002.

Grünewald, T., Bühler, Y., and Lehning, M.: Elevation dependency of mountain snow depth, The Cryosphere, 8, 2381–2394, https://doi.org/10.5194/tc-8-2381-2014, 2014.

Gobiet, A., Kotlarski, S., Beniston, M., Heinrich, G., Rajczak, J., Stoffel, M.: 21st century climate change in the European Alps—A review. Science of the Total Environment 493, 1138–1151, 2014.

Henderson, G. R., Peings, Y., Furtado, J. C. & Kushner, P. J.: Snow–atmosphere coupling in the Northern Hemisphere, Nature Climate Change. 8(11), 954-963, 10.1038/s41558-018-0295-6, 2018.

Hall, D. K. and Riggs, G.A.: MODIS/Terra Snow Cover Daily L3 Global 0.05Deg CMG, Version 6. Boulder, Colorado USA. NASA National Snow and Ice Data Center Distributed Active Archive Center. doi: https://doi.org/10.5067/MODIS/MOD10C1.006. (accessed on 15.08.2020), 2016.

Jacob, D., and Coauthors: Assessing the transferability of the regional climate model REMO to different CORDEX regions, Atmosphere, 3, 181-199, DOI:10.3390/atmos3010181, 2012.

Jonas, T., and Essery R.: Snow Cover and Snowmelt in Forest Regions. In: Singh V.P., Singh P., Haritashya U.K. (eds) Encyclopedia of Snow, Ice and Glaciers. Encyclopedia of Earth Sciences Series. Springer, Dordrecht. https://doi.org/10.1007/978-90-481-2642-2_499, 2014.

Jacob, D., Petersen, J., Eggert, B., Alias, A., Christensen, O. B., Bouwer, L. M., Braun, A., Colette, A., Déqué, M., Georgievski, G., Georgopoulou, E., Gobiet, A., Menut, L., Nikulin, G., Haensler, A., Hempelmann, N., Jones, C., Keuler, K., Kovats, S., Kröner, N., Kotlarski, S., Kriegsmann, A., Martin, E., van Meijgaard, E., Moseley, C., Pfeifer, S., Preuschmann, S., Radermacher, C., Radtke, K., Rechid, D., Rounsevell, M., Samuelsson, P., Somot, S., Soussana, J.-F., Teichmann, C., Valentini, R., Vautard, R., Weber, B. & Yiou, P.: EURO-CORDEX: new high-resolution climate change projections for European impact research, Regional Environmental Change. 14(2), 563-578, 10.1007/s10113-013-0499-2, 2014.

Jacob, D., Teichmann, C., Sobolowski, S. et al.: Regional climate downscaling over Europe: perspectives from the EURO-CORDEX community. Reg Environ Change **20,** 51. https://doi.org/10.1007/s10113-020-01606-9, 2020.

Kotlarski, S.: A Subgrid Glacier Parameterisation for Use in Regional Climate Modelling, Max-Planck Institut für Meteorologie Report No. **, 2007.

Lawrence, D. & Coauthors: Technical Description of version 5.0 of the Community Land Model (CLM), Boulder, CO, 329 pp, 2020.

Lüthi, S,. Ban, N., Kotlarski, S., Steger, C.R., Jonas, T., Schär, C.: Projections of Alpine Snow-Cover in a High-Resolution Climate Simulation. Atmosphere.; 10(8):463. https://doi.org/10.3390/atmos10080463, 2019.

Magnusson, J., Tobias, J., López-Moreno, I., Lehning, M.; Snow cover response to climate change in a high alpine and half-glacierized basin in Switzerland. Hydrology Research; 41 (3-4): 230–240. doi: https://doi.org/10.2166/nh.2010.115, 2010.

Matiu, M., Petitta, M., Notarnicola, C., Zebisch, M. Evaluating Snow in EURO-CORDEX Regional Climate Models with Observations for the European Alps: Biases and Their Relationship to Orography, Temperature, and Precipitation Mismatches. Atmosphere. 11(1):46. https://doi.org/10.3390/atmos11010046, 2020.

Matiu, M., Crespi, A., Bertoldi, G., Carmagnola, C. M., Marty, C., Morin, S., Schöner, W., Cat Berro, D., Chiogna, G., De Gregorio, L., Kotlarski, S., Majone, B., Resch, G., Terzago, S., Valt, M., Beozzo, W., Cianfarra, P., Gouttevin, I., Marcolini, G., Notarnicola, C., Petitta, M., Scherrer, S. C., Strasser, U., Winkler, M., Zebisch, M., Cicogna, A., Cremonini, R., Debernardi, A., Faletto, M., Gaddo, M., Giovannini, L., Mercalli, L., Soubeyroux, J.-M., Sušnik, A., Trenti, A., Urbani, S., and Weilguni, V.: Observed snow depth trends in the European Alps: 1971 to 2019, The Cryosphere, 15, 1343–1382, https://doi.org/10.5194/tc-15-1343-2021, 2021.

Mioduszewski, J.R., Rennermalm, A.K., Robinson, D.A., Wang, L. Controls on spatial and temporal variability in Northern Hemisphere terrestrial snowmelt timing, 1979-2012. Journal of Climate, 28 (6), pp. 2136-2153, 2015.

Moeser, D., Mazzotti, G., Helbig, N., and Jonas, T.: Representing spatial variability of forest snow: Implementation of a new interception model, Water Resour. Res., 52, 1208– 1226, doi:10.1002/2015WR017961, 2016.

Mooney, P. A., Lee, H., and Sobolowski, S.: Impact of quasi-idealized future land cover scenarios at high latitudes in complex terrain. Earth's Future, 9 (2), e2020EF001838. https://doi.org/10.1029/2020EF001838, 2021.

Muñoz Sabater, J.: ERA5-Land monthly averaged data from 1981 to present. Copernicus Climate Change Service (C3S) Climate Data Store (CDS). (accessed on 31.08.2020), 10.24381/cds.68d2bb30, 2019.

Muñoz-Sabater, J., Dutra, E., Agustí-Panareda, A., Albergel, C., Arduini, G., Balsamo, G., Boussetta, S., Choulga, M., Harrigan, S., Hersbach, H., Martens, B., Miralles, D. G., Piles, M., Rodríguez-Fernández, N. J., Zsoter, E., Buontempo, C., and Thépaut, J.-N.: ERA5-Land: A state-of-the-art global reanalysis dataset for land applications, Earth Syst. Sci. Data Discuss. [preprint], https://doi.org/10.5194/essd-2021-82, in review, 2021.

Niu, G.-Y., and Yang, Z.L.: The effects of canopy processes on snow surface energy and mass balances, J. Geophys. Res., 109, D23111, doi:10.1029/2004JD004884, 2004.

Niu, G.-Y., and Z.-L. Yang: An observation-based formulation of snow cover fraction and its evaluation over large North American river basins, J. Geophys. Res., 112, D21101, doi:10.1029/2007JD008674, 2007.

Niu, G. Y., & Coauthors: The community Noah land surface model with multiparameterization options (Noah-MP): 1. Model description and evaluation with local-scale measurements. Journal of Geophysical Research: Atmospheres, 116(D12), 2011.

Oleson, K. W., Lawrence, D. M., Bonan, G. B., Flanner, M. G., Kluzek, E., Lawrence, P. J., … Zeng, X.: Technical Description of version 4.0 of the Community Land Model (CLM) (No. NCAR/TN-478+STR). University Corporation for Atmospheric Research. doi:10.5065/D6FB50WZ, 2010.

Oleson K. W. & Coauthors: Technical description of version 4.5 of the Community Land Model (CLM). Boulder, CO, 420 pp, 2013.

Pomeroy, J.W., Gray, D.M., Shook, K.R., Toth, B., Essery, R.L.H., Pietroniro, A. and Hedstrom, N.: An evaluation of snow accumulation and ablation processes for land surface modelling. Hydrol. Process., 12: 2339-2367. https://doi.org/10.1002/(SICI)1099-1085(199812)12:15<2339::AID-HYP800>3.0.CO;2-L, 1998.

Roeckner, E., Arpe, K., Bentsson, L., Christoph, M., Claussen, M., Dümenil, L., Esch, M., Giorgetta, M., Schlese, U., and Schulzweida, U.: The atmospheric general circulation model ECHAM-

4: Model description and simulation of present day climate. Max-Planck Institut für Meteorologie Report No. 218, 90 pp, 1996.

Snyder, P.K., Delire, C. & Foley, J.A. Evaluating the influence of different vegetation biomes on the global climate. Climate Dynamics **23,** 279–302, https://doi.org/10.1007/s00382-004-0430-0, 2004.

Thackeray, C.W., Qu, X. and Hall, A.: Why do models produce spread in snow albedo feedback?. Geophysical Research Letters, 45(12), pp.6223-6231, 2018.

Qu, X., and A. Hall: What Controls the Strength of Snow-Albedo Feedback? J. Climate, **20,** 3971–3981, https://doi.org/10.1175/JCLI4186.1, 2007.

Qu X. and A. Hall: On the persistent spread in snow-albedo feedback. Clim Dyn, 42:69–81 DOI:10.1007/s00382-013-1774-0, 2014.

Reinhart V., Fonte C., Hoffmann P., Bechtel B., Rechid D., Böhner J.: Comparison of ESA Climate Change Initiative Land Cover to CORINE Land Cover over Eastern Europe and the Baltic States from a regional climate modeling perspective. Int. J. Earth Obs. 94, 102221. https://doi.org/10.1016/j.jag.2020.102221, 2020.

Rechid, D., Davin, E., de Noblet-Ducoudré, N., and Katragkou, E.: CORDEX Flagship Pilot Study LUCAS – Land Use & Climate Across Scales – a new initiative on coordinated regional land use change and climate experiments for Europe, in 19th EGU General Assembly, EGU2017, proceedings from the conference held 23–28 April, 2017 in Vienna, Austria, 19, p. 13172, 2017.

Rockel B., Will A. & Hense A.: The regional climate model COSMO-CLM (CCLM). Meteorologische Zeitschrift, 17(4), 347-348, 2008.

Roeckner E., Arpe K., Bentsson L., Christoph M., Claussen M., Dümenil L., Esch M., Giorgetta M., Schlese U. & Schulzweida U.: The atmospheric general circulation model ECHAM-4: Model description and simulation of present day climate. Max-Planck Institut für Meteorologie Report No. 218, 90 pp. , 1996.

Samuelsson, P., Gollvik S., Jansson, C., Kupiainen, M., Kourzeneva, E., & Jan van de Berg, W.: The surface processes of the Rossby Centre regional atmospheric climate model (RCA4). Reports METEOROLOGY, 157, SMHI, Norrköping, Sweden, 2015.

Samuelsson, P., Gollvik, S., & Ullerstig, A.: The land-surface scheme of the Rossby Centre regional atmospheric model (RCA3). Reports Meteorology, 122, SMHI, SE-60176 Norrköping, Sweden, 2006.

Schrodin, E., and Heise, E.: A new multi-layer soil model. COSMO Newsletter No. 2:149-151, 2002.

Skamarock, W. C., and Coauthors: A description of the advanced research WRF version 3, NCAR Technical Note. National Center for Atmospheric Research, Boulder, Colorado, USA, 2008.

Sofiadis, G., Katragkou, E., Davin, E. L., Rechid, D., de Noblet-Ducoudre, N., Breil, M., Cardoso, R. M., Hoffmann, P., Jach, L., Meier, R., Mooney, P., Soares, P. M. M., Strada, S., Tolle, M. H., and Warrach Sagi, K.: Afforestation impact on soil temperature in regional climate model simulations over Europe, Geosci. Model Dev. Discuss. [preprint], https://doi.org/10.5194/gmd-2021-69, in review, 2021.

Strandberg, G., Bärring L., Hansson U., Jansson C., Jones C., Kjellström E., Kolax M., Kupiainen M., Nikulin G., Samuelsson P., Ullerstig A. & Wang S.: CORDEX scenarios for Europe from the Rossby Centre regional climate model RCA4. SMHI Meteorology and Climatology Rep. 116, 84 pp., https://www.smhi.se/polopoly_fs/1.90275!/Menu/general/extGroup/attachmentColHold/mainCol1/file/RMK_116.pdf, 2015.

Sørland, S. L., Brogli, R., Pothapakula, P. K., Russo, E., Van de Walle, J., Ahrens, B., Anders, I., Bucchignani, E., Davin, E. L., Demory, M.-E., Dosio, A., Feldmann, H., Früh, B., Geyer, B., Keuler, K., Lee, D., Li, D., van Lipzig, N. P. M., Min, S.-K., Paniz, H.-J., Rockel, B., Schär, C., Steger, C., and Thiery, W.: COSMO-CLM Regional Climate Simulations in the CORDEX framework: a review, Geosci. Model Dev. Discuss. [preprint], https://doi.org/10.5194/gmd-2020-443, in review, 2021.

Tölle, M. H., M. Breil, K. Radtke, and H. J. Panitz: Sensitivity of European temperature to albedo parameterization in the regional climate model COSMO-CLM linked to extreme land use changes. Front. Environ. Sci., 6, 123, 10.3389/fenvs.2018.00123, 2018.

Verseghy, D.: CLASS—A Canadian land surface scheme for GCMs. I. Soil model. Int. J. Climatol. 11:111–133, 1991.

van Kampenhout, L., J.T.M. Lenaerts, W.H. Lipscomb, W.J. Sacks, D.M. Lawrence, A.G. Slater & M.R. van den Broeke: Improving the Representation of Polar Snow and Firn in the Community Earth System Model. Journal of Advances in Modeling Earth Systems 9, no. 7: 2583–2600. https://doi.org/10.1002/2017MS000988, 2017.

Wang A. & Zeng X.: Improving the treatment of the vertical snow burial fraction over short vegetation in the NCAR CLM3, Advances in Atmospheric Sciences. 26(5), 877-886, 10.1007/s00376-009-8098-3, 2009.

Wilhelm C., Rechid D. & D. Jacob: Interactive coupling of regional atmosphere with biosphere in the new generation regional climate system model REMO-iMOVE. Geoscientific Model Development, 7(3), 1093-1114, 2014.

Xu, L., & Dirmeyer, P.: Snow–Atmosphere Coupling Strength. Part I: Effect of Model Biases, Journal of Hydrometeorology. 14(2), 389-403, 10.1175/jhm-d-11-0102.1, 2013a.

Xu, L., & Dirmeyer, P.: Snow–Atmosphere Coupling Strength. Part II: Albedo Effect Versus Hydrological Effect, Journal of Hydrometeorology, 14(2), 404-418, 2013b.

Xu, L., and Dirmeyer, P.: Snow-atmosphere coupling strength in a global atmospheric model, Geophys. Res. Lett., 38, L13401, doi:10.1029/2011GL048049, 2011.

Ye, H. and Cohen, J.: A shorter snowfall season associated with higher air temperatures over northern Eurasia, Environmental Research Letters, 8, 014052, doi:10.1088/1748-9326/8/1/014052, 2013.

Figures and Tables
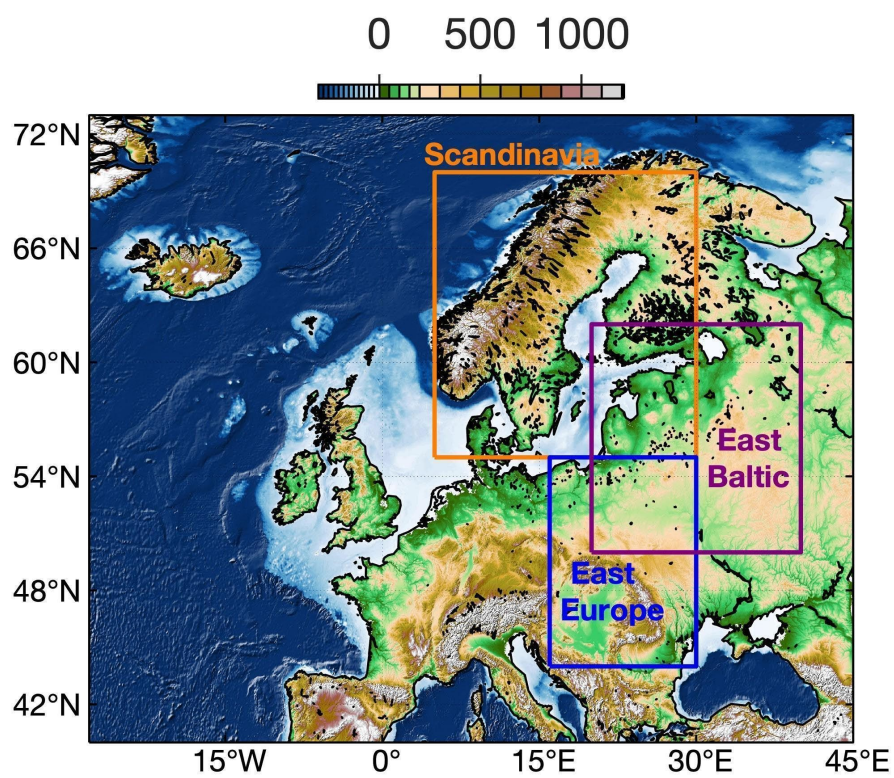
Figure 1: Map showing the location of the three regions of interest: Scandinavia (orange), East Baltic (purple) and East Europe (blue).
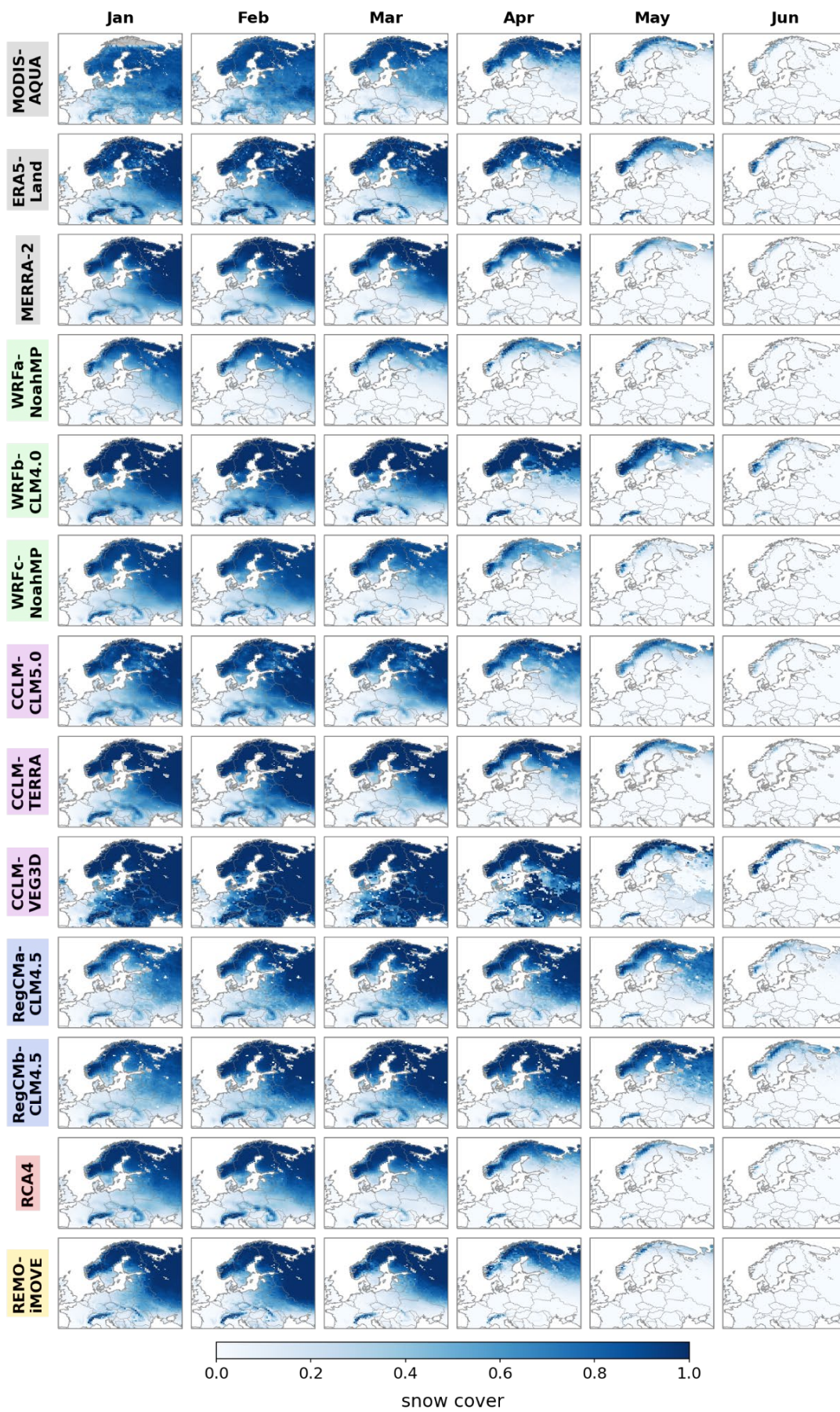
Figure 2: Spatial maps of snow cover for the satellite observations MODIS-AQUA, the reanalyses ERA5-Land and MERRA2, and the ten RCMs from the EVAL experiment of LUCAS. Data show monthly averages from January to June over the period 1986-2015 for models and reanalyses and over 2003-2015 for satellite observations. See Figure S2 in the supplemental material for the same figure will all datasets averaged over the time period 2003-2015.
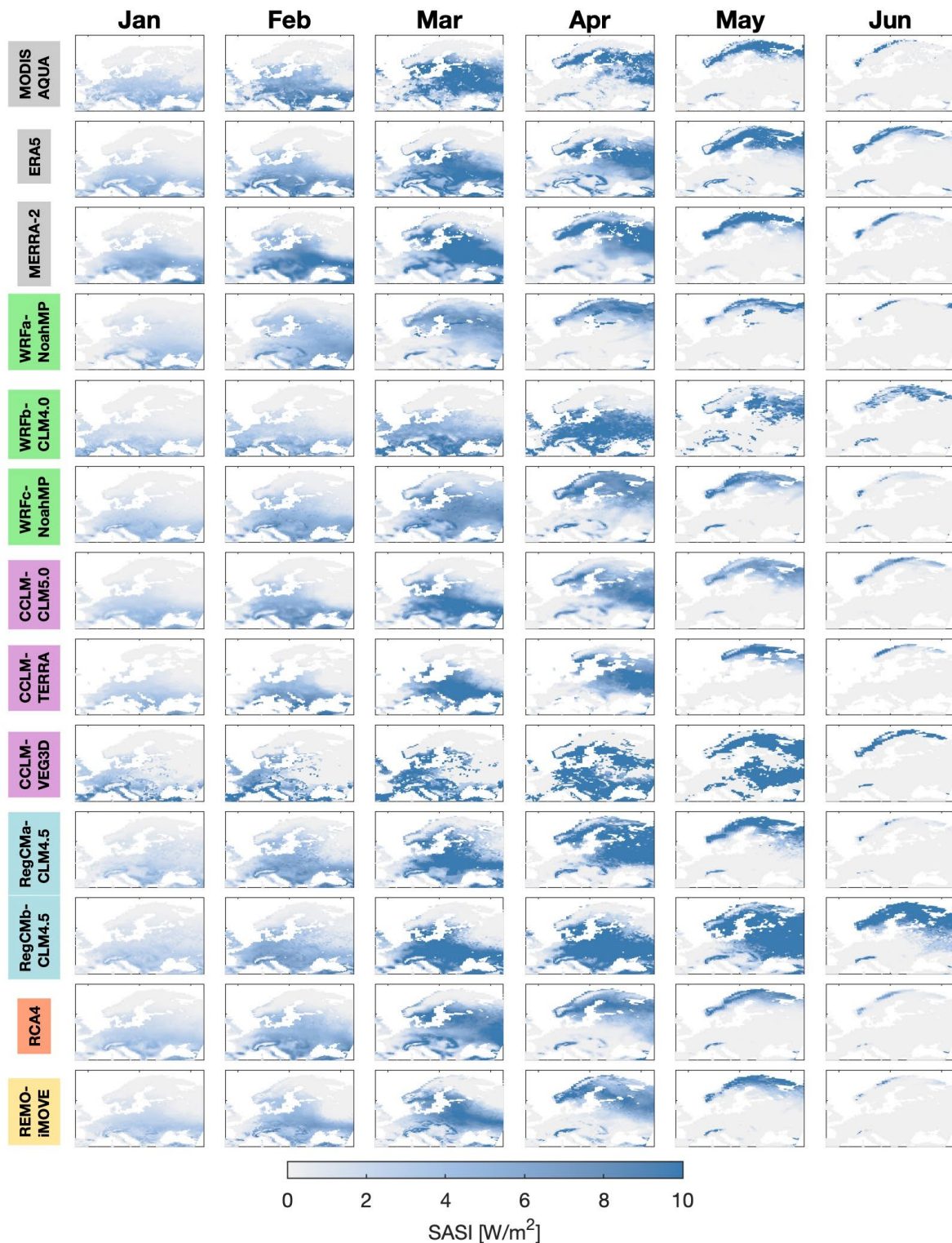
Figure 3: Spatial maps of SASI (Wm^{-2}) for satellite observations (MODIS-AQUA), the reanalysis ERA5-Land and the ten RCMs from the EVAL experiment of LUCAS from January to June, averaged over the time period 1986-2015.
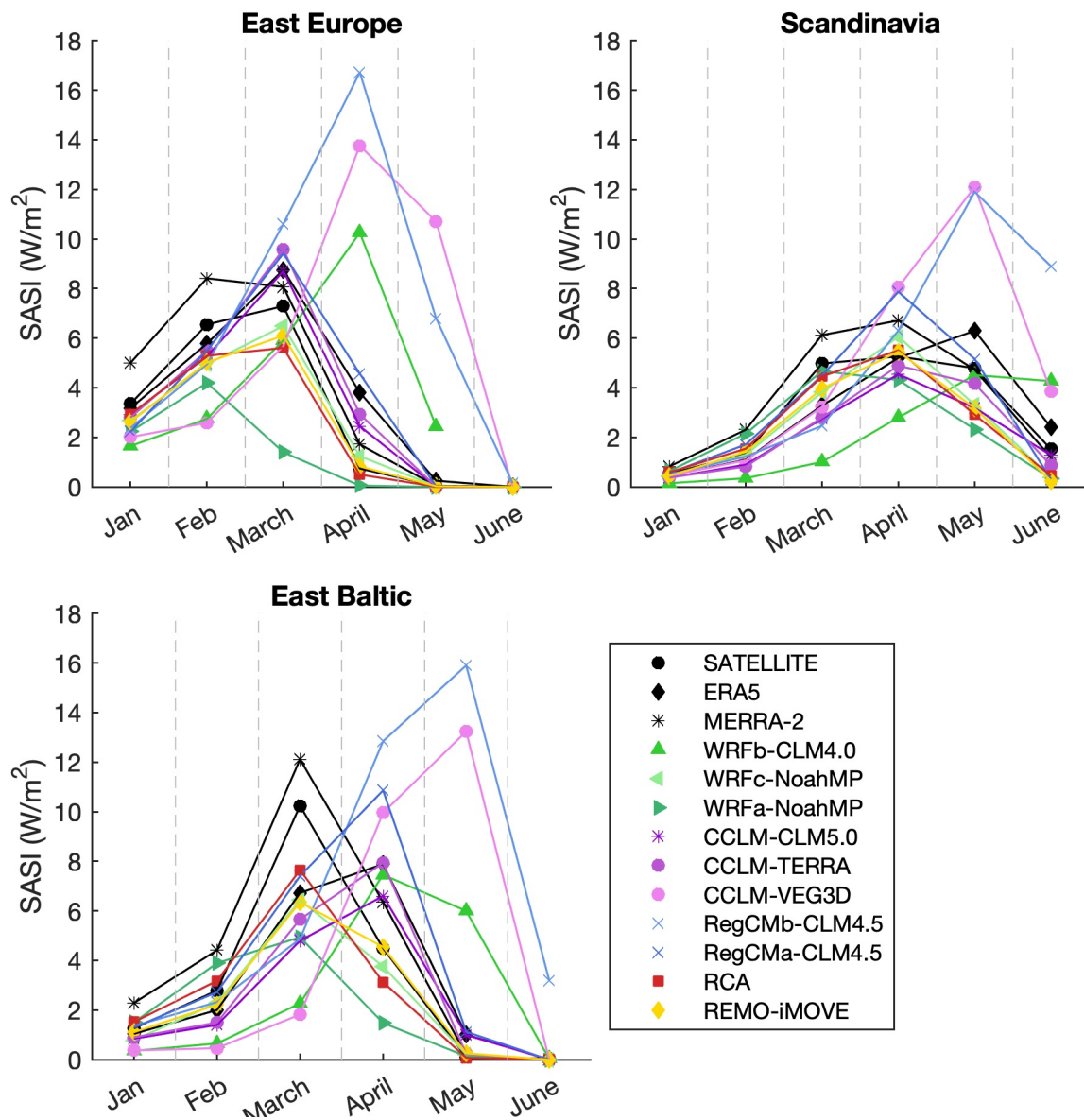
Figure 4: Time series of the spatial average of SASI for the satellite observations, the reanalysis ERA5-Land and the ten RCMs from the EVAL experiment of LUCAS in Scandinavia, East Europe and East Baltic (see Figure 1 for their spatial extent). Data are averaged over the time period 1986-2015.
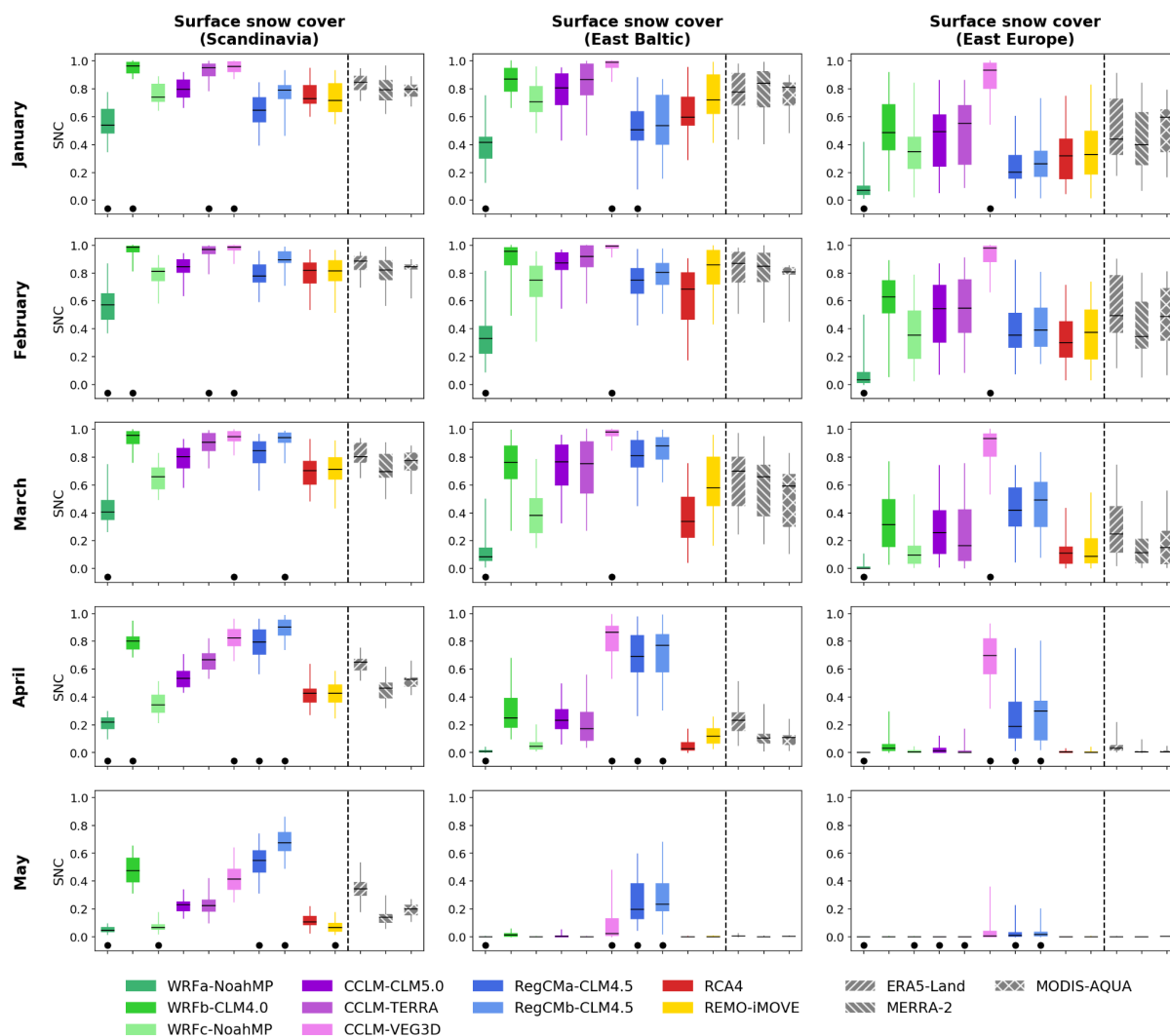
Figure 5: Snow cover for the 10 RCMs, the reanalyses ERA5-Land and MERRA-2, and the satellite observations MODIS-AQUA for January to May. The box-and-whisker-plots show the interannual variability of snow cover over 1986-2015 for models and reanalyses and over 2003-2015 for satellite observations. Bars represent the median, boxes the interquartile range, and whiskers the minimum/maximum values. Dots indicate models lying outside the range of the reference datasets MERRA-2, ERA5-Land, and MODIS-AQUA, i.e., the 25th (75th) model percentile is higher (lower) than the highest 75th (lowest 25th) quantile of the reference datasets. For satellite observations we only use data from days and pixels with less than 50% cloud cover. See Figure S1 for in the supplemental material for the same figure including data for MODIS displayed for cloud cover fraction thresholds of 50% and 20%.
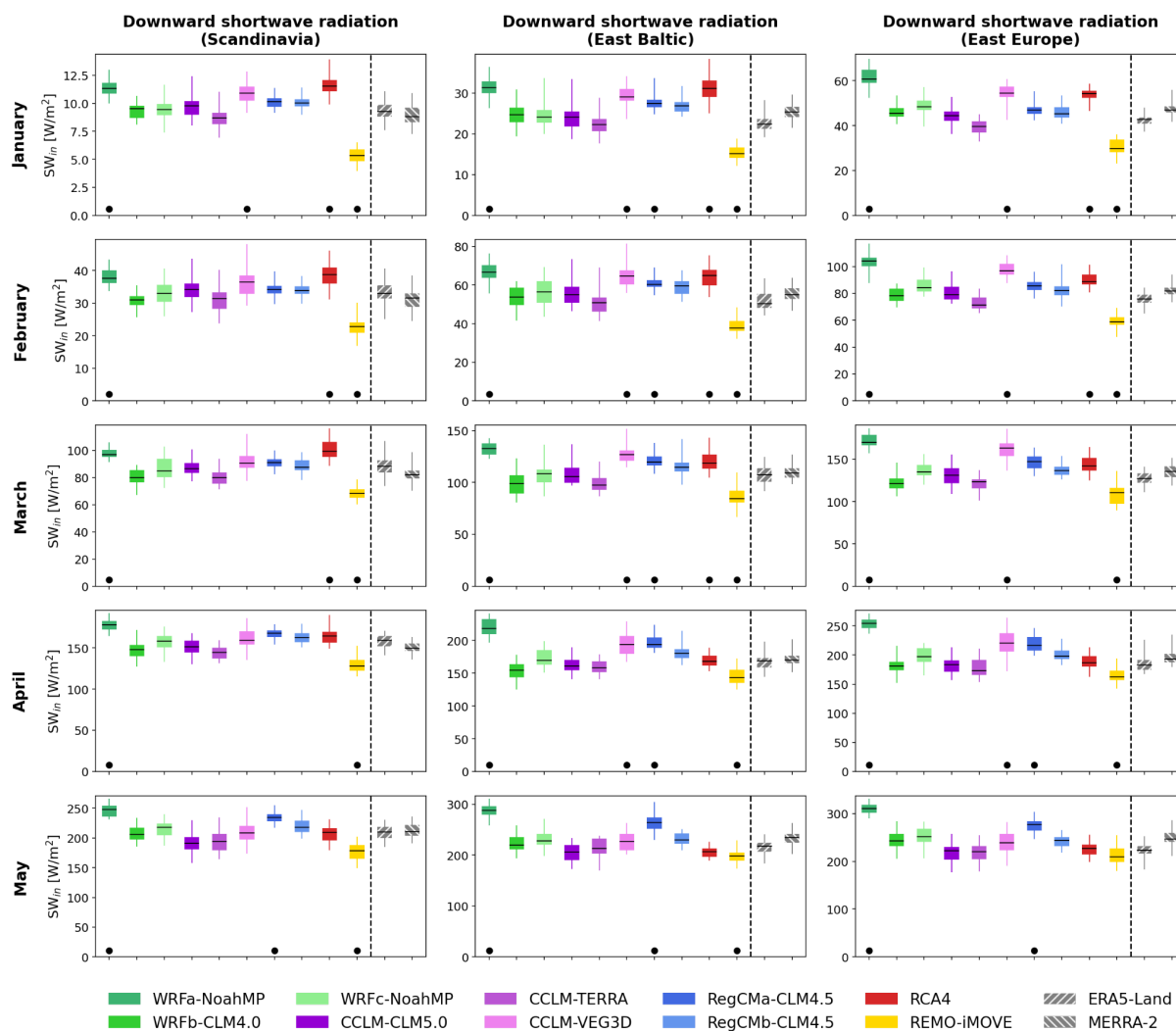
Figure 6: Downward surface shortwave radiation for the 10 RCMs for MERRA-2, and ERA5-Land, for January to May. The box-and-whisker-plots show the interannual variability of downward shortwave radiation over 1986-2015, with the bar representing the median, boxes the interquartile range, and whiskers the minimum/maximum values. Dots indicate models lying outside the range of the reference datasets MERRA-2, ERA5-Land, and MODIS (i.e., the 25th (75th) model percentile is higher (lower) than the highest 75th (lowest 25th) quantile of the reference datasets). See Figure S5 in the supplemental material for the same figure will all datasets averaged over the time period 2003-2015.
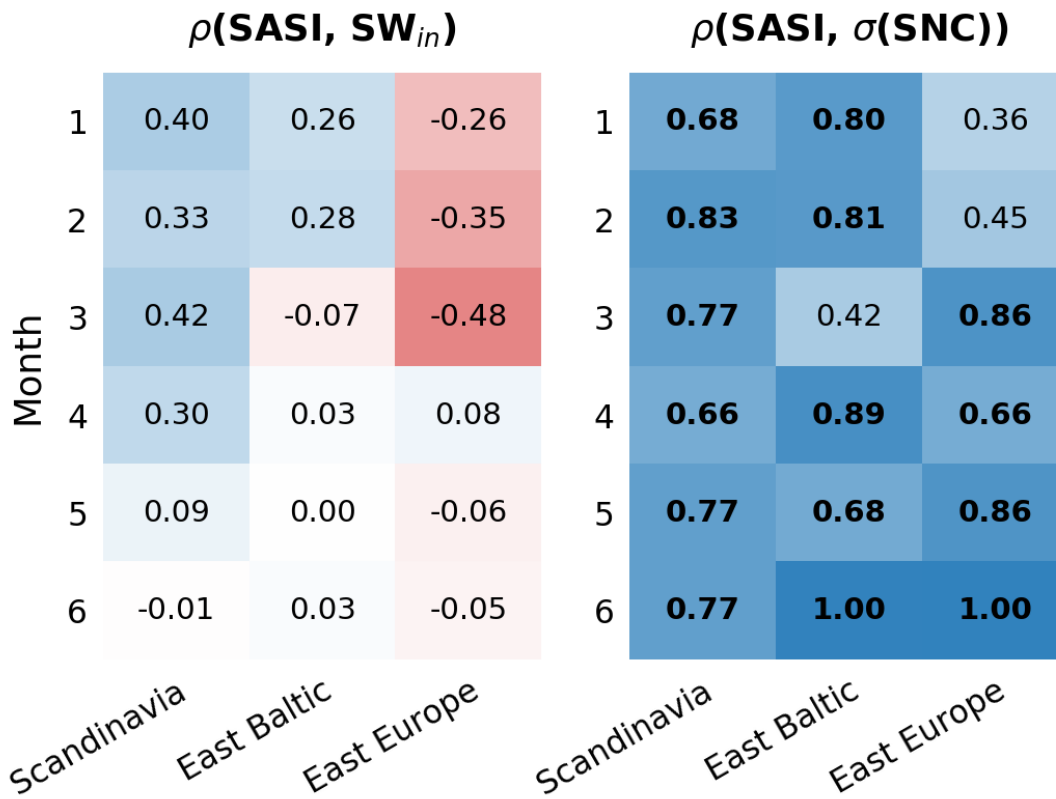
Figure 7: Pearson correlation between SASI and shortwave radiation (left), and SASI and standard deviation of snow cover (right) calculated across RCMs for the three regions Scandinavia, East Baltic, and East Europe for the months January to June during 1986-2015. The values represent the variable (shortwave radiation or variability in snow cover) to which the inter-model variability of SASI is predominantly related to. Bold values indicate statistical significance at the 0.05 level (two-tailed p-value).

Name of the models	RCM	LSM	Representation of sub-grid scale surface heterogeneity	Phenology	Snow-vegetation interaction	Institute ID
WRFa-NoahMP	WRF v3.8.1D [Skamarock et al., 2008]	NoahMP [Niu et al., 2011]	PFT-dominant	Prescribed	Deardorff, 1978; Niu and Yang, 2007	IDL
WRFb-CLM4.0	WRF v3.8.1 [Skamarock et al., 2008]	CLM4.0 [Oleson et al., 2010]	PFT-tile	Prescribed	Wang and Zeng, 2009	AUTH
WRFc-NoahMP	WRF v3.8.1 [Skamarock et al., 2008]	NoahMP [Niu et al., 2011]	PFT-dominant	Prescribed	Deardorff, 1978; Niu and Yang, 2007	BCCR
CCLM-CLM5.0	Cosmo_5.0_clm9 [Soerland et al., 2021]	CLM5.0 [Lawrence et al., 2020]	PFT-tile	Prescribed	Wang and Zeng, 2009; Lawrence et al., 2020; van Kampenhout et al., 2017	ETH
CCLM-TERRA	Cosmo_5.0_clm9 [Soerland et al., 2021]	TERRA-ML [Schrodin and Heise, 2002]	PFT-dominant	Prescribed	Doms et al., 2013	CLMcom-JLU
CCLM-VEG3D	Cosmo_5.0_clm9 [Soerland et al., 2021; Rockel et al., 2008]	VEG3D [Braun and Schädler, 2005]	PFT-dominant	Prescribed	Grabe, 2002	KIT
RegCMa-CLM4.5	RegCM v4.6 [Giorgi et al., 2012]	CLM4.5 [Oleson et al., 2013]	PFT-tile	Prescribed	Wang and Zeng, 2009	ICTP
RegCMb-CLM4.5	RegCM v4.7 [Giorgi et al., 2012]	CLM4.5 [Oleson et al., 2013]	PFT-tile	Prescribed	Wang and Zeng, 2009	CUNI
RCA4	RCA4 [Strandberg et al., 2015]	Internal [Samuelsson et al., 2006]	PFT-tile	Prescribed	Samuelsson et al., 2015	SMHI
REMO-iMOVE	REMO2009 [Jacob et al., 2012]	iMOVE [Wilhelm et al., 2014]	PFT-tile	Interactive	Roeckner et al., 1996; Kotlarski, 2007	GERICS

Table 1: Summary of participating regional climate models and their land surface models.